

# Structure and dynamics of 9-ethylfluorene-Ar<sub>n</sub> van der Waals complexes

Jonathan D. Pitts and J. L. Knee<sup>a)</sup>

Department of Chemistry, Wesleyan University, Middletown, Connecticut 06459

(Received 28 August 1998; accepted 27 October 1998)

The neutral  $S_1$  excited state and the ion ground state of 9-ethylfluorene-Ar<sub>n</sub> van der Waals complexes have been studied for  $n=1-3$ . Resonance enhanced multiphoton ionization spectroscopy of the  $S_1$  state of the argon clusters reveals multiple isomeric structures for each of the cluster sizes studied coupled with the two monomer conformations. The  $n=1$  cluster shows three isomers, one of the symmetric 9-ethylfluorene and two of the unsymmetric. The  $n=2$  clusters has four possible isomers all of which are assigned to a (1|1) conformation, although each represents a unique structure with different argon binding sites. The  $n=3$  cluster collapses down to two dominate isomers, one for each conformation of the parent. Mass analyzed threshold ionization (MATI) spectroscopy was used to investigate the ion, as well as assisting in isomer assignment of the  $S_1$  spectrum. IVR and dissociation of the argon complexes have also been studied with MATI spectroscopy. *Ab initio* calculations are used to determine the binding energy for all conformers and isomers of the  $n=1$  complex. These values are in excellent agreement with the experimentally bracketed values, and prove useful in isomer assignments. Redistribution of the 208 cm<sup>-1</sup> band of the  $n=2$  symmetric conformation shows dynamics suggesting interconversion of all isomers to a new unassigned structure. Preferential dissociation of the argon located on the ethyl chain side of the sym-9-ethylfluorene-Ar<sub>2</sub> complex is observed in both isomers. © 1999 American Institute of Physics. [S0021-9606(99)01405-1]

## I. INTRODUCTION

Perhaps one of the most fundamental properties of molecular clusters is their geometry. A detailed understanding of cluster geometry is essential to the prediction of reactivity as well as dynamical processes. In an attempt to further our understanding of van der Waals cluster dynamics and reactivity, the 9-ethylfluorene-Ar<sub>n</sub> (EF-Ar<sub>n</sub>) ( $n=1-3$ ) system has been studied. This study is motivated by previous work on fluorene<sup>1,2</sup> and 9-phenylfluorene<sup>3</sup> in which we were able to observe multiple isomers for a single cluster size. Phenylfluorene formed a rich variety of these isomers, presumably due to the asymmetry introduced with respect to the ‘‘top’’ and ‘‘bottom’’ side of the ring system. The presence of these multiple isomers then allows one to study isomer specific properties. We are particularly interested in measuring the differences in dynamics including energy redistribution and cluster dissociation. 9-ethylfluorene (EF) provides an asymmetry similar to phenylfluorene and was indeed found to form multiple isomers. One of the more interesting features of this molecule is the multiple conformations of the ethyl side chain. In the preceding article<sup>4</sup> it was shown that two stable conformations of 9-ethylfluorene exist in the beam which differ in the orientation of the ethyl side chain with respect to the ring. The most abundant conformer was determined to have the ethyl chain pointing back to the ring forming a symmetric structure (sym). The less stable conformer has the ethyl chain rotated  $\sim 120^\circ$  forming an unsymmetric structure (unsym). Each of these conformations can

form van der Waals complexes with argon giving additional possibilities to measure structure specific properties.

Conformational studies of large organic molecules constitute a significant area of research both experimentally and computationally. Nuclear magnetic resonance (NMR),<sup>5</sup> x-ray crystal structures,<sup>5,6</sup> microwave,<sup>7,8</sup> infrared spectroscopes,<sup>8</sup> and photoelectron spectroscopy<sup>9</sup> have all been used to characterize the geometries and interactions of monomers,<sup>4-7</sup> oligomers,<sup>7</sup> and complexes<sup>7-9</sup> of various molecules. Equally significant is the computational effort. Molecular dynamics,<sup>10</sup> as well as *ab initio*<sup>11</sup> methods have provided a wealth of information on such systems. Still there is much to be learned about these systems, such as characterizing structure specific dynamical processes like dissociation and IVR.

The presence of multiple conformations in molecular beams is well characterized. Multiple conformations for systems such as alkylbenzenes<sup>12</sup> and alkylanilines,<sup>13</sup> styrene,<sup>14</sup> *p*-dimethoxybenzene,<sup>15</sup> etc. have been studied previously. In all cases, each conformation has a unique  $S_1$  origin and ionization potential. Similarly, multiple isomeric structures for a given cluster size have been observed.<sup>2,16</sup> Interestingly enough, little work has been done that combines these two features into a single molecular system. Kimura *et al.* show the existence of the *cis* and *trans* *p*-dimethoxybenzene-Ar<sub>n</sub> ( $n=1,2$ ) but due to the molecules planarity only a single isomer is seen for each rotamer.<sup>15</sup> Recent studies by our group have shown that multiple isomers may exist even for small cluster sizes.<sup>4</sup> In the case of 9-phenylfluorene-Ar<sub>n</sub> multiple isomers exist for clusters as small as  $n=1$ . This would lead one to believe that a combination of isomers and conformers may exist in the jet.

With this objective in mind, 9-ethylfluorene was selected

<sup>a)</sup>Electronic mail: jknee@wesleyan.edu

due to its two conformations<sup>4</sup> and its reduced symmetry (with respect to the unsubstituted fluorene) in both the symmetric and unsymmetric conformations. To date no work has been done on the argon clusters. Itoh and Morita<sup>17</sup> published results on the exciplex formation of  $(EF)_2$ . These results present fluorescence spectra and decay times of the monomer and dimer, as well as comparisons to fluorene dimer and the heterocluster of fluorene and EF. Additionally, Itoh and Hayashi<sup>18</sup> studied the complexation of EF with methyl-substituted dienes. Again they report excitation spectra and lifetime measurements of the complexes. Finally, Auty, Jones, and Phillips report the excitation spectra of  $EF^{19}$  monomer. Here they assign the excitation spectra as consisting of only one conformation with the monomer lifetime measured as 121 ns.

## II. EXPERIMENT

A detailed description of the experimental apparatus has been given elsewhere,<sup>1</sup> so only a brief abridgment is given here. Two color 1+1 resonance enhanced multiphoton ionization (REMPI) spectroscopy with mass resolved detection is used to study the spectroscopy of the  $S_1$  electronic state of the jet-cooled clusters. Mass analyzed threshold ionization (MATI) spectroscopy,<sup>20</sup> the mass resolved equivalent of zero electron kinetic energy (ZEKE) spectroscopy, is used for the photoelectron spectroscopy of the ion ground state. References 1–4 and 21 give a complete description of our application of ZEKE and MATI to the study of molecular clusters.

Nanosecond and picosecond laser systems were separately used in this study. The nanosecond laser system employed in these experiments consists of two dye lasers (Lumonics HD-500) pumped by the second harmonics of a pulsed Nd:yttrium–aluminum–garnet (YAG) (Continuum NY-61) operating at 20 Hz. The visible output of the each dye laser has a pulse width of 6 ns and a bandwidth of  $0.04\text{ cm}^{-1}$ . Both dye lasers are frequency doubled and one functions as the pump and the other as the probe. The pump and probe lasers were temporally overlapped by an appropriate optical delay and spatially overlapped in the vacuum chamber under slightly focused conditions. Care was taken to minimize any signal from either laser alone. The second laser system used for time resolved studies is a pulse amplified picosecond system. This consists of a continuous wave mode-locked Nd:YAG (Coherent Antares) synchronously pumping two dye lasers. Each dye laser is amplified in separate three stage dye amplifiers, pumped by the second harmonic of a Nd:YAG regenerative amplifier (Continuum RGA-67) operating at 22 Hz. The amplified output pulse width is  $\sim 15\text{ ps}$  with a bandwidth of  $5\text{ cm}^{-1}$  and an energy of  $0.2\text{--}1\text{ mJ/pulse}$  in the visible. The overall cross correlation is  $>20\text{ ps}$  due to jitter between the two dye lasers. Laser wavelengths were calibrated with a Na/K/Ne hollow cathode lamp.

A pulsed supersonic beam originates in the first of two differentially pumped chambers. The nozzle has a sample container which holds the EF sample (Aldrich) and is heated to  $110\text{--}150^\circ\text{C}$ . The exact vapor pressure is unknown but we estimate it as significantly below 1 Torr. For complexation of

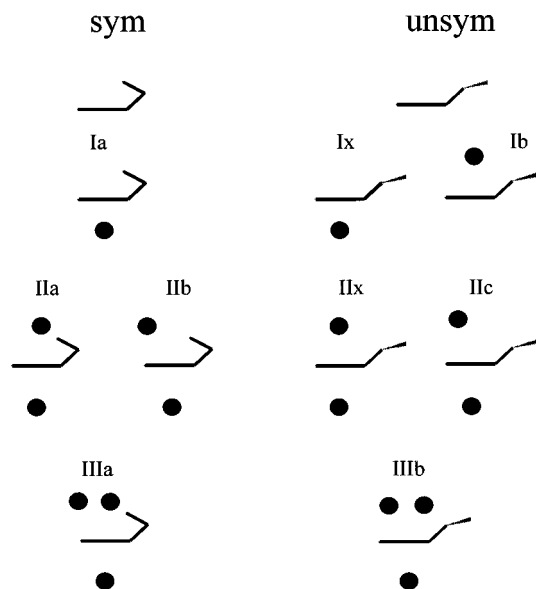


FIG. 1. Schematic representations of the  $EF-Ar_n$  ( $n=0\text{--}3$ ) system. The filled circles represent argon atoms. The assigned isomer nomenclature is indicated above each structure.

EF with Ar, a mixture of 10% or 20% Ar in He or Ar in Ne was used in the expansion. The backing pressure was varied from 1.4 to 2.5 bar in order to optimize the desired clusters. The pulsed beam is skimmed and enters the second chamber where the spectroscopy takes place.

The REMPI spectra were obtained by fixing the probe slightly higher than the ionization potential of the complex and scanning the pump. Probe energy and intensity were adjusted to avoid any dissociation from higher clusters. The MATI spectra were obtained by fixing the pump to the  $S_1$  vibronic band of interest and scanning the probe through the ionization potential (IP). To achieve clean separation of the prompt and MATI signals we implemented a pulsed Wiley–McClaren<sup>22</sup> extraction scheme in which the upper grid pulse width was varied to act as a mass filter. In this way the contribution from the cluster and fragments, other than the one of interest, could be eliminated. The MATI scheme used a delayed discrimination field of  $-3\text{ V/cm}$  and an extraction pulse of  $800\text{ V/cm}$  which was delayed  $\geq 10\text{ }\mu\text{s}$ . The ions then traverse the time-of-flight (TOF) mass spectrometer and are detected on dual stack microchannel plates (Galileo Electro-Optic Corp).

## III. RESULTS

### A. $S_1$ spectroscopy

#### 1. EF monomer

The spectroscopy of the monomer is discussed in the preceding article so only a brief summary of the information pertinent to our cluster discussion is given herein. The monomer exhibits two conformations as seen in Fig. 1 and listed in Table I (a detailed view is shown in Fig. 1 of Ref. 4). These have been assigned<sup>4</sup> to the symmetric (sym) and unsymmetric (unsym) conformations with their band origins at  $33\,543$  and  $33\,663\text{ cm}^{-1}$ , respectively. The symmetric conformation has the ethyl chain rotated back toward the five

TABLE I. Summary of EF-Ar<sub>n</sub> (*n*=0–3) spectra data. All values in cm<sup>-1</sup>.

Species	<i>S</i> <sub>1</sub>		<i>S</i> <sub>1</sub> →ion <sup>a</sup>	Δ( <i>S</i> <sub>1</sub> →ion) <sup>a</sup>	IP <sup>b</sup>	ΔIP <sup>a</sup>	
	Origin <sup>a</sup>	Δ <i>S</i> <sub>1</sub> <sup>a</sup>					
<i>n</i> =0	sym	33 543	–	29 688	–	63 231	–
	unsym	33 663	+120	29 488	–200	63 151	–80
<i>n</i> =1	sym- <b>Ia</b>	33 497	–46	29 652	–36	63 149	–82
	unsym- <b>Ix</b>	33 607	–56	29 463	–25	63 070	–81
	unsym- <b>Ib</b>	33 639	–24	29 446	–42	63 085	–66
<i>n</i> =2	sym- <b>IIa</b>	33 477	–66	29 637	–51	63 114	–117
	sym- <b>IIb</b>	33 513	–30	29 563	–125	63 076	–155
	unsym- <b>IIX</b>	33 582	–81				
	unsym- <b>IIc</b>	33 606	–57	29 419	–69	63 025	–126
<i>n</i> =3	sym- <b>IIIa</b>	33 490	–53	29 555	–133	63 045	–186
	unsym- <b>IIIb</b>	33 549	–114	29 395	–93	62 944	–207

<sup>a</sup>Experimental accuracy of ±1 cm<sup>-1</sup>.<sup>b</sup>Experimental accuracy of ±3 cm<sup>-1</sup>.

membered ring of the fluorene. This forms a *C*<sub>s</sub> symmetry structure with the mirror plane containing the ethyl carbons and bisecting the fluorene through the five membered ring, perpendicular to the fluorene plane. The unsymmetric conformation has the ethyl chain pointing away from the fluorene with a dihedral angle of –70°.

## 2. EF-Ar<sub>n</sub> (*n*=1–3) spectra and isomer assignment

Mass resolved resonance enhanced multiphoton ionization (REMPI) spectroscopy was used to study the first excited singlet state of the EF-Ar<sub>n</sub> (*n*=0–3). Figure 2 shows the excitation spectrum near the origin region of all clusters studied and Table I summarizes the *S*<sub>1</sub> resonances. For the *n*=1 complex, both the symmetric and unsymmetric conformers continue to be present in the molecular beam. The ratio of the unsymmetric to symmetric for the *n*=1 is similar to the ratio for the monomer, 0.17 and 0.18, respectively.

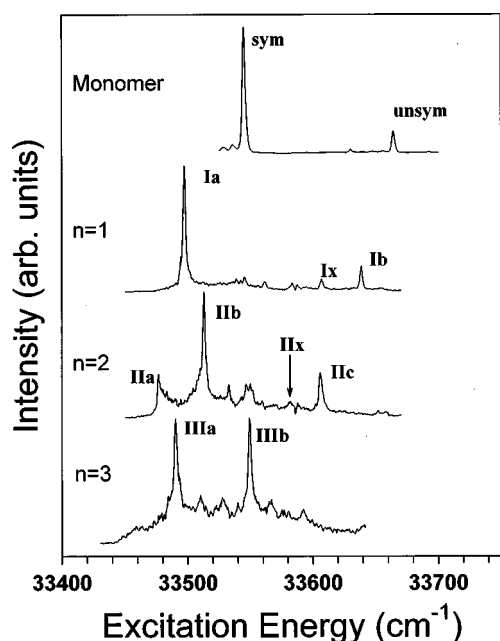


FIG. 2. EF-Ar<sub>n</sub> (*n*=0–3) mass gated resonance enhanced MPI spectra of the *S*<sub>1</sub> state. The respective isomer *S*<sub>1</sub> origins are labeled. In all cases the probe energy was fixed just above the IP so as to avoid ion fragmentation.

The *n*=1 complex of the sym conformer is red shifted by 46 cm<sup>-1</sup> and the *n*=1 complex of the unsym conformers is red shifted by 24 cm<sup>-1</sup> from their respective monomer origins. Additionally a third *n*=1 isomer is seen associated with the unsymmetric conformation. This band, although weak, can be unambiguously assigned as a separate isomer due to its unique ionization potential (see text below as well as Table I). This band is red shifted from the corresponding monomer origin by 56 cm<sup>-1</sup>. According to standard additivity rules, one would assign the sym-EF-Ar complex as having the argon on the side opposite the ethyl chain (**Ia**). This assignment comes from comparing the *S*<sub>1</sub> shift to that of fluorene-Ar,<sup>1</sup> which is, 42 cm<sup>-1</sup> and by analogy to 9-phenylfluorene-Ar.<sup>3</sup> Similarly the two isomers of the unsymmetric conformation (unsym-EF-Ar) can be assigned as one on the side opposite the ethyl chain (**Ix**) and one on the side with the ethyl chain (**Ib**). The first being the most red shifted (56 cm<sup>-1</sup>) origin and the later being the less red shifted (24 cm<sup>-1</sup>) origin. The **Ix** nomenclature is chosen because these isomers are only studied in the excited state, and used for isomer assignment, their intensity limits the experimental opportunities for MATI spectroscopy. These conformations are represented schematically in Fig. 1.

The EF-Ar<sub>2</sub> excitation spectrum is shown in Fig. 2. Here one clearly sees at least three peaks corresponding to three different origins. The reddest of these at 33 477 cm<sup>-1</sup> corresponds to an isomer of the symmetric conformation (**IIa**). The most intense peak at 33 513 cm<sup>-1</sup> also corresponds to an *n*=2 isomer of the symmetric conformation (**IIb**), although different than the first one, as will be revisited in the discussion section. Additionally there is an origin band assigned to the *n*=2 unsymmetric conformer (**IIc**). It is known from IP selective REMPI that a second conformation of the unsym-EF-Ar<sub>2</sub> complex exists with its *S*<sub>1</sub> origin at 33 582 cm<sup>-1</sup> (**IIX**) but its small intensity limits the experimental possibilities. Using the additivity rules as above, one would expect any additional red shift, relative to the *n*=1 cluster, to imply that the new argon is binding to a side opposite the first argon. In the case of the **IIa** isomer this would suggest a (1|1) conformation. The other symmetric isomer, **IIb**, is blue shifted from the *n*=1 symmetric isomer origin. This implies a breakdown of the additivity rules. For reasons to be discussed below, this isomer has been assigned as a (1|1) structure, but having the second argon in a significantly different place than the second argon of **IIa**. The unsymmetric **IIX** isomer is red shifted from the **Ix** isomer by 25 cm<sup>-1</sup> and thus bears a striking resemblance to the **Ib** isomer shift of –24 cm<sup>-1</sup>. This **IIX** origin value (Table I) is determined from probe selective REMPI spectra that enhance the **IIX** signal level over the background. Here the additivity rules apply and the **IIX** is assigned to the (1|1) configuration (**Ib**+**Ix**) of the unsymmetric conformation. Finally the **IIc** isomer is again red shifted from the **Ib** isomer, but only by 33 cm<sup>-1</sup>. In accordance with the additivity rules, this isomer is also assigned to a (1|1) structure. Here though, the second argon is in a place that causes only a small perturbation to the *S*<sub>1</sub> origin. Again this seems similar to the **IIb** structure where the second argon occupies the side with the ethyl chain, but in a less favorable spot than the **IIa** or **IIX**. See Fig. 1 for a

schematic representation of all the  $n=2$  complexes. An important observation to make is that the  $n=2$  REMPI spectrum has somewhat broad peaks and an underlying background. This is taken to suggest that other conformations exist in the molecular beam that are not resolvable in these experiments.

The  $n=3$  REMPI spectrum also show features due to the symmetric (**IIIa**) and unsymmetric (**IIIb**) conformations of EF. This is confirmed by the determination of the ionization potential using MATI spectroscopy (see Table I). The **IIIa** isomer is red shifted by  $23\text{ cm}^{-1}$  from the **IIb**. This shift is similar to the unsym-EF-Ar (**Ib**) isomer. Although we do not know the shift for the sym-EF-Ar where the argon is on the ethyl chain side, the similarity to the unsymmetric case leads this isomer to be assigned as a (2|1) structure with the argon dimer on the side with the ethyl chain. The **IIIb** isomer is red shifted from the **IIc** isomer by  $57\text{ cm}^{-1}$ . This shift is identical to the **Ix** shift, again suggesting that the third argon is on the side with the ethyl chain. As in the case of  $n=2$ , the  $n=3$  REMPI exhibits a large background indicative of a continuum of unresolved structures. This is consistent with an increase in cluster size.<sup>2,3</sup>

## B. Ion spectroscopy

### 1. Monomer MATI spectroscopy

In an attempt to understand the dynamics and geometry of the EF-Ar<sub>n</sub> system, the MATI spectra at the origin and at higher  $S_1$  vibronic intermediates were obtained. A detailed analysis of the monomer MATI is undertaken in Ref. 1, so again only a brief summary of the information relevant to the cluster discussion is given here.

The MATI spectra obtained by pumping the  $S_1$  origins of the monomer are shown in Fig. 3 and summarized in Table I. As alluded to above, pumping the band at  $33\,543\text{ cm}^{-1}$  produces a sharp peak at  $29\,688\text{ cm}^{-1}$ . This is assigned to the symmetric isomer and an ionization potential of  $63\,230.7\text{ cm}^{-1}$  is determined. Similarly by pumping the excitation band at  $33\,663\text{ cm}^{-1}$  a strikingly different MATI spectrum is obtained. The main feature,  $\Delta v=0$ , in this spectrum is centered at  $29\,488\text{ cm}^{-1}$ . This measures a significantly different IP of  $63\,151\text{ cm}^{-1}$ . This band is assigned to the origin of the unsymmetric conformation (see Fig. 3).

### 2. Cluster MATI

$n=1$ : The MATI spectra obtained by pumping the  $n=1$  symmetric and unsymmetric conformations are seen in Fig. 3. The position of these bands are listed in Table I. By pumping the three excitation bands previously assigned to the different isomers **Ia**, **Ix**, and **Ib**, one obtains different MATI spectra and hence different ionization potentials, confirming the existence of the three isomers. In addition, the MATI spectra show a red shift in the **Ia** IP of  $82\text{ cm}^{-1}$  (Table I) which is similar to the fluorene-Ar IP shift<sup>1</sup> of  $-93\text{ cm}^{-1}$  as well as the 9-phenylfluorene-Ar IP shift<sup>3</sup> of  $-79\text{ cm}^{-1}$ . This helps in confirming the structural assignment above since addition to the ethyl chain side would presumably have a different effect on the IP. Similarly, an IP shift for the **Ix** isomer of  $81\text{ cm}^{-1}$  is recorded (Table I). This

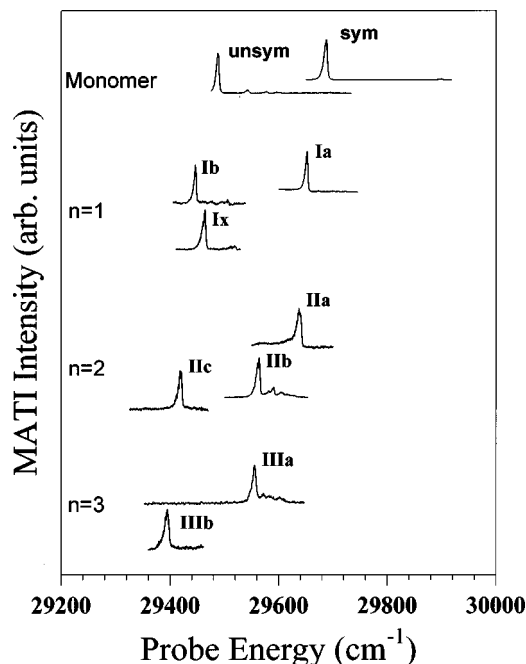


FIG. 3. MATI spectra of EF-Ar<sub>n</sub> clusters from  $n=0$  to 3. The spectra were obtained by pumping the respective  $S_1$  origin labeled next to each peak and scanning the probe through the ionization potential. The MATI spectra are plotted as a function of probe energy.

would suggest the addition of the argon to the fluorene like side of EF, and indeed this is the assignment given above. Finally the IP shift for the **Ib** isomer is  $-66\text{ cm}^{-1}$ . This is significantly different than the **Ia** or **Ix**, implying that the argon is on the side of the ethyl chain. This is in direct agreement with the assignment from the excitation spectra.

Several other MATI spectra for the  $n=1$  cluster were obtained by pumping higher energy excitation bands and recording the MATI signal in the region of the  $\Delta v=0$  transition. The behavior of EF-Ar seems to be similar to that of fluorene-Ar. That is we see little or no redistribution occurring at low energy ( $208\text{ cm}^{-1}$ ). The first band for which we see significant redistribution occurring is at  $398\text{ cm}^{-1}$  excess energy. The redistribution is characterized by a broadening of the MATI spectrum in the  $\Delta v=0$  region with an associated red shift, presumably due to lowering of the van der Waals mode frequencies in the cation. This MATI signature of cluster redistribution is well characterized in fluorene-Ar<sub>n</sub>,<sup>1,2</sup> phenylfluorene-Ar<sub>n</sub><sup>3</sup> and other systems.<sup>21</sup> The next highest band in the  $S_1$  spectrum of the EF-Ar complex is assigned to the sym-EF-Ar  $514\text{ cm}^{-1}$  band. This band again shows significant redistribution on the nanosecond time scale. Both of these bands are seen in Fig. 4. While the exact temporal evolution of the IVR of these band was not measured, the nanosecond evolution at fixed delays [early (1 ns) and late time (7 ns)] was recorded. All MATI bands measured above this, when gating on the  $n=1$  mass, are assigned to dissociation products in the excited state of the  $n=2$  complex. This allows us to place a lower limit of  $514\text{ cm}^{-1}$  on the  $S_1$  binding energy of the Ar. This is in good agreement with fluorene-Ar,<sup>15</sup> which is bracketed between 410 and  $593\text{ cm}^{-1}$ .

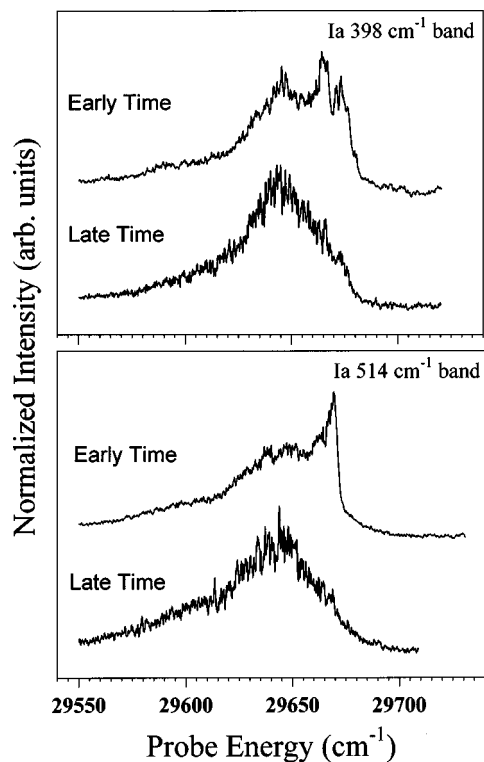


FIG. 4. The nanosecond MATI spectra of EF-Ar pumping the 398 (top) and 514  $\text{cm}^{-1}$  (bottom)  $S_1$  bands. The spectra are scanned in the  $\Delta\nu=0$  region. Early time corresponds to an optical delay of  $<1$  ns, late time corresponds to a delay of 7 ns. The broad structure to the red is indicative of IVR occurring at the expense of the sharp reactant structure.

$n=2$ : Of significantly more interest is the EF-Ar<sub>2</sub> MATI. Figure 3 shows the MATI spectra pumping the origins of the two conformations, and the isomers of each conformation. As was the case above, the differences in the MATI spectra allows us to unambiguously assign the conformers origin resonances.

Figure 5 shows the nanosecond MATI spectra recorded by pumping the 208  $\text{cm}^{-1}$  bands of the two isomers (**IIa** and **IIb**) of the sym conformation. In each case IVR is seen as a broad peak shifted from the sharp structure. In the case of the **IIa** isomer, the redistribution occurs to the red of the sharp reactant peak. This is a standard shift for the redistributed product as described above for the  $n=1$  complexes. The **IIb** isomer on the other hand shows a dramatic blue shift of the redistributed product. This is very uncharacteristic of these systems. In an attempt to better understand this phenomenon picosecond MATI spectra were recorded for both of these bands. These are shown in Fig. 6. As one can see there is only sharp structure occurring at early time (zero ps), and significant redistribution as the probe laser is delayed relative to the excitation. The temporal evolution of the reactant decay was monitored for both isomers. They show a similar rate of redistribution of  $\sim 475$  ps (see insets of Fig. 6). The 208  $\text{cm}^{-1}$  band of the unsymmetric conformation shows only broad structure on the nanosecond time scale even at early time. This suggests a very fast rate of redistribution. Due to lack of signal intensity this band could not be measured with the time resolved picosecond system. Still one can conclude that the redistribution is faster in the unsymmetric conforma-

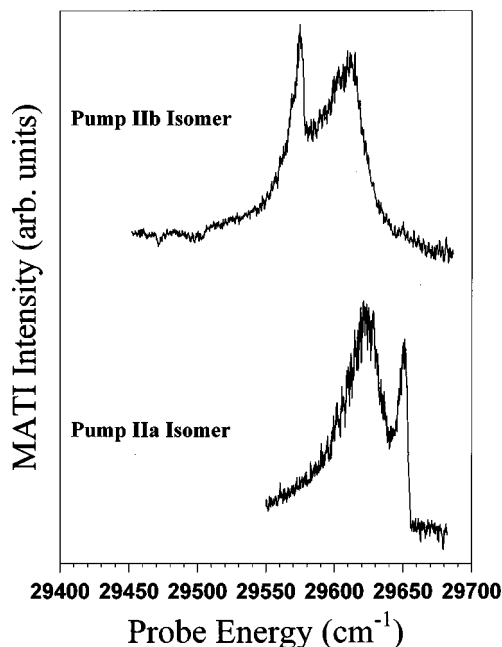


FIG. 5. The nanosecond MATI spectra of the EF-Ar<sub>2</sub> cluster pumping the  $S_1$  208  $\text{cm}^{-1}$  band. Both isomers, **IIb** (top) and **IIa** (bottom) show redistribution upon excitation.

tion than in the symmetric. This is an example of conformer specific redistribution rates.

Another point of interest in the  $n=2$  complex involves the dissociation of an argon from the complex. A number of bands were studied at various energies above the conformers respective origins and the MATI spectra recorded in the

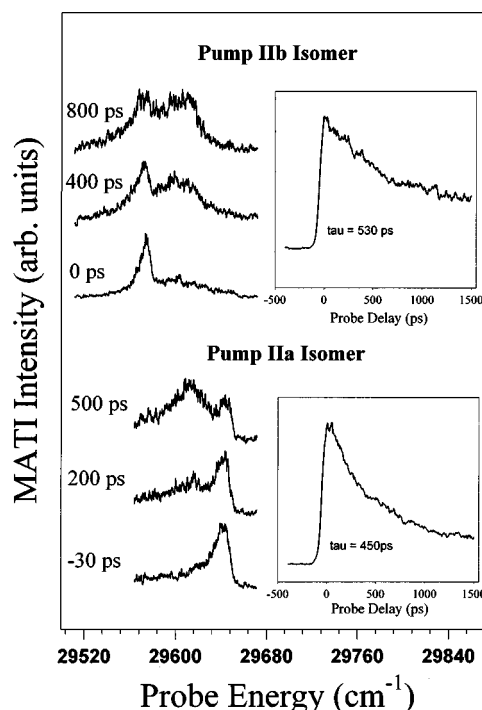


FIG. 6. The picosecond MATI spectra of the EF-Ar<sub>2</sub> cluster pumping the  $S_1$  208  $\text{cm}^{-1}$  band. Both isomers **IIb** (top) and **IIa** (bottom) show dynamical redistribution. The initial state decay is shown in the insets, which are obtained by monitoring the sharp structure in the MATI spectra.

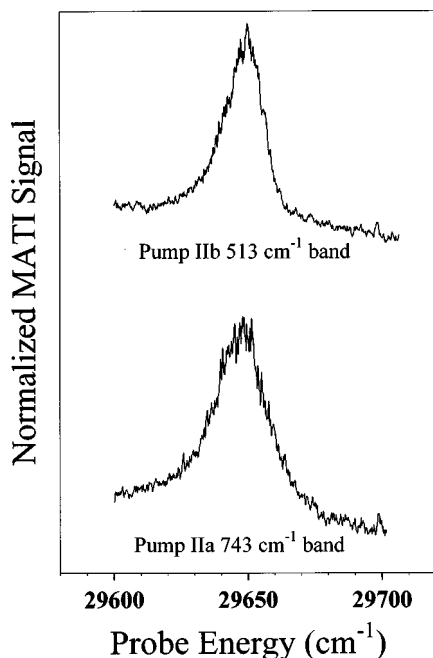


FIG. 7. Dissociation product MATI of the  $n=2$  complex. The pump is resonant with a  $n=2$   $S_1$  band above the dissociation threshold and the product MATI is monitored in the  $n=1$  mass channel.

$\Delta v=0$  region. To record dissociation using MATI spectroscopy the pump is tuned to an  $n=2$   $S_1$  resonance above the dissociation threshold, and the product is monitored in the  $n=1$  mass channel. The  $S_1$  bands include the 513, 669, 713, and 742  $\text{cm}^{-1}$ . The MATI of these bands were recorded for both the **IIa** and **IIb** isomers, i.e., both isomers of the sym conformer. Due to lack of signal, high-energy MATI spectra of the unsymmetric conformer were difficult to obtain. The onset of dissociation for the sym-EF-Ar<sub>2</sub> complex occurs at 513  $\text{cm}^{-1}$  in both isomers. This allows us to bracket the dissociation of a single argon in the sym-EF-Ar<sub>2</sub> complex between 398 and 513  $\text{cm}^{-1}$ . As an example of the nanosecond MATI spectra of dissociation products, see Fig. 7. All of the product MATI for the various dissociating intermediate states of both symmetric isomers occurs at 29 647  $\text{cm}^{-1}$  as shown in the figure.

#### IV. CALCULATIONS

To predict the geometry of the EF-Ar<sub>n</sub> system a series of molecular dynamics and structure minimization calculations using the HyperChem<sup>23</sup> package were undertaken. Similar calculations have been performed in the past by our group.<sup>1-3</sup> Briefly, a 6-12 Lennard-Jones potential is used to describe the nonbonded interactions between the argon and the chromophore, as well as between the argons themselves. The parameters describing these interactions are given in Ref. 1. To calculate the geometry of various clusters, a simulated annealing process was performed on each cluster. Leaving the EF fixed in its geometry as determined by *ab initio* methods<sup>4</sup> the argons are heated to between 50 and 100 K and allowed to sample the phase space freely. After adequate sampling, the cluster is quenched back to zero Kelvin. It is then geometry optimized, and the structure and energy

TABLE II. EF-Ar<sub>n</sub> calculated isomers and binding energies.

Cluster	Isomer	$L$ - $J$ energy ( $\text{cm}^{-1}$ ) <sup>a,c</sup>	<i>Ab-initio</i> energy ( $\text{cm}^{-1}$ ) <sup>b,c</sup>
unsym-EF-Ar	<b>Ix</b>	-518	-573
sym-EF-Ar	<b>Ia</b>	-511	-567
unsym-EF-Ar	<b>Ib</b>	-542	-498
unsym-EF-Ar	(1 0)	-563	-497
unsym-EF-Ar	(1 0)	-539	-486
sym-EF-Ar	(1 0)	-584	-467
unsym-EF-Ar <sub>2</sub>	(1 1)	-1060	
unsym-EF-Ar <sub>2</sub>	<b>IIc</b>	-1063	
unsym-EF-Ar <sub>2</sub>	(0 2)	-1063	
sym-EF-Ar <sub>2</sub>	(0 2)	-1067	
unsym-EF-Ar <sub>2</sub>	<b>IIx</b>	-1084	
sym-EF-Ar <sub>2</sub>	<b>IIa</b> or <b>IIb</b>	-1098	
sym-EF-Ar <sub>2</sub>	(2 0)	-1130	
unsym-EF-Ar <sub>2</sub>	(2 0)	-1203	

<sup>a</sup>Relative to the monomer energy (0  $\text{cm}^{-1}$ ), for the appropriate conformer. The EF is optimized with B3LYP (6-31G\*).

<sup>b</sup>B3LYP (6-31G\*) optimized EF. 6-31+G\*\* basis centered on the EF and 6-311++G(2df,2dp) basis centered on argon. BSSE counterpoise correction included, see the text.

<sup>c</sup>Neglecting zero point energy.

recorded. Each conformation of each cluster size undergoes hundreds of annealing/optimization processes to ensure all local minima are found.

The calculations predict four minimum energy isomers for the unsym-EF-Ar cluster and two for the sym-EF-Ar cluster. Additionally five unsym-EF-Ar<sub>2</sub> clusters and three sym-EF-Ar<sub>2</sub> clusters are predicted from these calculations. Table II gives a summary of the calculated conformations and their energy.

While these calculations are useful, it was realized that the binding energy results of these simple calculations did not agree with experiment. It would be advantageous to have a much higher level of theory to make quantitative statements about relative energies and binding energies. Several types of calculations and experimental techniques have been used to bracket binding energies in numerous systems. Here we use quantum MP2 calculations (GAUSSIAN 94)<sup>24</sup> to predict the binding energy of the sym and unsym-EF-Ar complex. The total geometry optimization of the EF-Ar complex with basis sets capable of describing such a system is computationally beyond our means at present. To circumvent this limitation, we chose to use the B3LYP optimized parent with the argon placement predicted by the above Lennard-Jones calculations. To test the accuracy of this method, we chose benzene-Ar as a test system. This system is particularly useful because both experimental<sup>25</sup> and MP2 calculated<sup>11,26,27</sup> binding energies are available.

The first calculation was our own full optimization of the benzene-Ar system. This was performed at the MP2 level of theory using a 6-31+G(*d,p*) basis set on the benzene and a 6-311++G(2df,2dp) basis set centered on the argon atom. These large basis sets have been shown to accurately describe the interactions present in these van der Waals complexes.<sup>26</sup> Additionally one must account for the error in the calculated binding energy caused by basis set superposi-

tion error (BSSE). This is described by Boys and Bernardi,<sup>28</sup> and their method of correcting this error is implemented here and in all other cluster calculations presented. In these calculations, the chromophore is fixed in its optimized geometry. In the case of benzene, this is at the MP2 level. Additionally a frozen core approximation is used. Our calculations predict a binding energy of the fully optimized (MP2) benzene-Ar of 413 cm<sup>-1</sup>. This is in excellent agreement with the value calculated by Schlag *et al.*<sup>11</sup> of 429 cm<sup>-1</sup>. Now the MP2 optimized benzene chromophore is fixed and the argon placement is determined by the simple Lennard-Jones type calculations described above. Using this new cluster, (whose geometry is very similar to the full MP2 calculated geometry) a single-point energy calculation of the energy is performed at the same level of theory used in the MP2 fully optimized benzene-Ar. The total energy of the full MP2 structure and the molecular mechanics placed argon have nearly identical values (i.e., the Lennard-Jones structure is only 2.6 cm<sup>-1</sup> lower). These results are promising in that we will be able to accurately predict binding energies of large van der Waals systems (specifically the EF-Ar complex) using this computationally simpler method.

To that end, the calculation of the binding energy of EF-Ar was undertaken. As was noted before, it was computationally infeasible for us to perform a full MP2 optimization on this system. Similarly, it was infeasible to optimize just the EF parent at the MP2 level. However, due to the approximations used in density functional calculations accurate geometries of both the sym and unsym-EF were obtained.<sup>4</sup> We will use these optimized parents as the fixed chromophore in the method described for the benzene-Ar. Unfortunately density functional theory (DFT) has not proven useful in predicting the binding energy of van der Waals systems consistently.<sup>29</sup> The same 6-31+G(*d,p*)/6-311++G(2*df*,2*dp*) basis set combination was used. In the case of the unsym-EF-Ar there were four conformations predicted in the simulated annealing/optimization procedure, described above. The binding energy of all four of these conformations were calculated and the results are shown in Table II. Additionally there were two conformations of the sym-EF-Ar. These calculated binding energies are also shown in Table II.

The calculations predict, in both the sym and unsym-EF-Ar that the argon located on the side opposite the ethyl chain has the highest binding energy, 567 and 573 cm<sup>-1</sup>, respectively. The zero point energy of the EF-Ar system was not calculated, and is neglected in these reported values, but can be estimated as similar to the benzene-Ar value of 50 cm<sup>-1</sup>.<sup>11</sup> The particular value of the zero point energy is not critical since it is expected to be similar for each isomer and thus does not effect the relative binding energies of the different isomers. As was noted above, the experimental *S*<sub>1</sub> binding energy for the *n*=1 complex is >514 cm<sup>-1</sup>. The calculated values of the ground state binding energy of a single argon are consistent with this lower limit. Similarly the dissociation of a single argon from the *n*=2 complex is experimentally bracketed between 398 and 513 cm<sup>-1</sup>. In fact, the value for dissociation of a single argon from the *n*=2 complex can also be predicted by the *n*=1 calculation

of the binding energies (498–467 cm<sup>-1</sup>). In this case, one must assume that the argon dissociates from the ethyl chain side (see below), and that the argon–argon interactions are negligible if the argons are on opposite sides of the parent molecule.

## V. DISCUSSION

As was seen in the ion spectroscopy section, the two isomers of the sym-EF-Ar<sub>2</sub> show redistribution upon excitation to 208 cm<sup>-1</sup>. As seen in Figs. 5 and 6, the redistribution of the **IIb** isomer uncharacteristically redistributes to the blue, while the **IIa** shows a “normal” redistribution to the red. The characteristic red shifted IVR is a result of population of bath states, after excitation, associated with the 208 cm<sup>-1</sup> vibration. The anomalous blue shift of the **IIb** isomer is taken to suggest that the redistributed product starts to sample one or more different isomeric structures. In fact, the MATI spectrum resulting from this “new” isomer is quite similar to the normal, red shifted structure present in the redistribution of the **IIa** isomer excited to the same *S*<sub>1</sub> band, Fig. 5. It is concluded that **IIb** is starting to sample the same, or similar, isomer structures as **IIa**. Remember that **IIa** and **IIb** are proposed to differ only in the position of an Ar on the “top,” ethyl side of the ring. It is reasonable to expect that at 208 cm<sup>-1</sup> the Ar is able to overcome barriers for moving on the surface of the molecule, although the surface crossing barrier is likely to be higher, as was the case in fluorene-Ar<sub>3</sub>. Rather than considering the redistributed Ar to be a specific isomer structure it is more likely that both **IIa** and **IIb** are sampling many possible structures on the surface of the fluorene, which on the average give the broad MATI signal shown in Figs. 5 and 6.

In a converse argument this phenomenon helps in the assignment of the isomeric geometry. Since **IIa** and **IIb** appear to be able to interconvert at 208 cm<sup>-1</sup>, yet surface crossing is not possible, it requires that **IIa** and **IIb** both be either (2|0) or (1|1) structures. In accordance with the additivity rules (see isomer assignments above) the **IIa** and **IIb** complexes are most likely (1|1).

Dissociation of the *n*=2 complex also helps to assign structures to the different isomers. As seen in Fig. 7, dissociation from either the **IIa** or **IIb** isomer result in identical product MATI spectra. These spectra are coincident with the MATI spectra of the **Ia** isomer excited above the *S*<sub>1</sub> origin as shown in Fig. 4. In other words the products of the *n*=2 dissociation, both **IIa** and **IIb**, are essentially identical to the redistributed **Ia** isomer. Again assuming that upon dissociation, surface crossing is unlikely, at the excess energy investigated, the **IIa** and **IIb** isomers must represent similar initial structures. If one, according to the additivity rules, is to assign the **IIa** to the (1|1) conformation one must conclude that the **IIb** is also a (1|1) conformation. This is in direct agreement with the results of the 208 cm<sup>-1</sup> band. In addition to the starting conformation one knows which argon is favored in the dissociation since the final structure is **Ia**, a structure with the argon on the side opposite the ethyl chain. That is, the argon on the same side as the ethyl chain must be removed. Dissociation of the argon from the ethyl chain side of the molecule is also supported by the *ab initio* calculation of

the binding energy. It is predicted that the argon on the ethyl chain side always has a lower binding energy ( $466\text{ cm}^{-1}$ ) than the argon on the side without the ethyl group ( $567\text{ cm}^{-1}$ ). This adds support to the above isomer assignments. It is noted that the **IIa** and **IIb** isomers must be similar (1|1) structures, but the argon on the ethyl chain side must exist in two spectrally different orientations. This is in agreement with the REMPI results predicting **IIa** and **IIb** to have similar (1|1) structures, but the argon on the ethyl chain side occupies two inequivalent positions. The Lennard-Jones calculations above predict only a single (1|1) structure. It is quite possible that other isomers exist at this excess energy that are not represented in the atom-atom calculations, and would all be higher in energy than the ones predicted by the annealing/optimization process.

In addition it is noted that the  $S_1$  dissociation energy of the symmetric  $n=1$  complex (**Ia**) is  $>514\text{ cm}^{-1}$ . This is higher than the  $S_1$  dissociation energy of the  $n=2$  complex which is bracketed between  $398$  and  $514\text{ cm}^{-1}$ . This observation suggests that the dissociation of the argon added to the ethyl chain side is more easily facilitated than the fluorene like side. In fact the calculated binding energies for the ethyl chain side of EF are all below  $500\text{ cm}^{-1}$ , and the binding energies of the argon opposite the ethyl group are all greater than  $514\text{ cm}^{-1}$ . Again this is consistent with the isomer assignments above based on the understanding that addition to an identical side of the molecule would be nearly additive in argon dissociation energy between the  $n=1$  and 2 clusters. This observation supports the accuracy of the *ab initio* calculations prediction of the binding energy. All of the calculated values fall well within the experimentally bracketed values.

## VI. CONCLUSION

The 9-ethylfluorene- $\text{Ar}_n$  system has been studied in both the excited state, and the ion. The  $S_1$  REMPI spectroscopy reveals two conformations of the parent, and multiple isomers of the EF- $\text{Ar}_n$  ( $n=1-3$ ). From standard additivity rules, the geometry of the  $n=1-3$  clusters is determined. The MATI spectroscopy of the ion assists in the determination of geometry as well as allowing for determination of the binding energy of the  $n=1$  and 2 complex. The binding energy is experimentally bracketed for the  $n=1$  as  $>514\text{ cm}^{-1}$  and the  $n=2$  as  $398-513\text{ cm}^{-1}$ .

The dynamics of the sym-EF- $\text{Ar}_2$  complex shows redistribution at an excess energy of  $208\text{ cm}^{-1}$ . The two isomers of this cluster redistribute to a similar unresolved structure. This implies that the two isomers must have similar (1|1) reactant structures. The dissociation of the sym-EF- $\text{Ar}_2$  complex produces a single  $n=1$  product. This product is always the **Ia** conformation.

Molecular dynamics and *ab initio* calculations were performed to predict the geometry and binding energy of the EF- $\text{Ar}_n$  clusters. There is a discrepancy in the binding energy calculated by atom-atom empirical calculations vs that calculated by the MP2 algorithm. After comparison to experiment, it was determined that the *ab initio* calculations accurately predicted the binding energy. The *ab initio* calculations predict the argon on the side opposite the ethyl chain to

be the most tightly bound. This is consistent with the experimental dissociation results that show the **IIa** and **IIb** isomers always yielding the **Ia** conformer upon dissociation.

## ACKNOWLEDGMENT

We gratefully acknowledge the NSF for financial support of this project under Grant No. CHE-9523575.

- <sup>1</sup>X. Zhang, J. D. Pitts, R. Nadarajah, and J. L. Knee, *J. Chem. Phys.* **107**, 8239 (1997).
- <sup>2</sup>J. D. Pitts and J. L. Knee, *J. Chem. Phys.* **108**, 9632 (1998).
- <sup>3</sup>J. D. Pitts and J. L. Knee, *J. Chem. Phys.* (in press).
- <sup>4</sup>J. D. Pitts and J. L. Knee, *J. Chem. Phys.* **110**, 3378 (1999), preceding paper.
- <sup>5</sup>J. S. Davies, J. R. Everett, I. K. Hatton, E. Hunt, J. W. Tyler, I. I. Zomaya, A. M. Z. Slawin, and D. J. Williams, *J. Chem. Soc., Perkin Trans. 2* **2**, 201 (1991).
- <sup>6</sup>M. Mori, K. Okada, K. Shimazaki, T. Chuman, S. Kuwahara, T. Kitahara, and K. Mori, *J. Chem. Soc., Perkin Trans. 1* **6**, 1769 (1990); K. Rang, E. Liao, J. Standstrom, and S. Wang, *J. Chem. Soc., Perkin Trans. 2* **7**, 1521 (1995); T. Nevalainen, K. Rissanen, *J. Chem. Soc., Perkin Trans. 2* **2**, 271 (1994).
- <sup>7</sup>K. R. Leopold, G. T. Fraser, S. E. Novick, and W. Klemperer, *Chem. Rev.* **94**, 1807 (1994); S. E. Novick, *Bibliography of Rotational Spectra of Weakly Bound Complexes*, 1998 (unpublished); Electronic updates are available from the author upon request at snovick@wesleyan.edu and on the World Wide Web at <http://www.wesleyan.edu/chem/bios/vdw.html>.
- <sup>8</sup>S. Tseng, D. F. Eggers, T. A. Blake, R. Beck, R. O. Watts, F. J. Lovas, and N. Zobov, *J. Mol. Spectrosc.* **182**, 132 (1997).
- <sup>9</sup>R. Sussmann, U. Zitt, and H. J. Neusser, *J. Chem. Phys.* **101**, 9257 (1994); W. L. Meerts, W. A. Majewski, and W. M. van Herpen, *Can. J. Phys.* **62**, 1293 (1984).
- <sup>10</sup>T. Troxler and S. Leutwyler, *J. Chem. Phys.* **99**, 4363 (1993); S. Leutwyler and J. Bosiger, *Chem. Rev.* **90**, 489 (1990); N. Ben-Hoein, U. Even, and J. Jortner, *J. Chem. Phys.* **97**, 5989 (1992); P. Parneix, P. Brechignac, and F. Amar, *J. Chem. Phys.* **104**, 983 (1996).
- <sup>11</sup>P. Hobza, O. Bludsky, H. L. Selzle, and E. W. Schlag, *J. Chem. Phys.* **97**, 335 (1992); S. Scheiner, *Molecular Interactions, From van der Waals to Strongly Bound Complexes* (Wiley, West Sussex, England, 1997), and references therein.
- <sup>12</sup>J. B. Hopkins, D. E. Powers, and R. E. Smalley, *J. Chem. Phys.* **72**, 5039 (1980); J. B. Hopkins, D. E. Powers, S. Mukamel, and R. E. Smalley, *J. Chem. Phys.* **72**, 5049 (1980); J. B. Hopkins, D. E. Powers, and R. E. Smalley, *J. Chem. Phys.* **73**, 683 (1980); M. Takahashi and K. Kimura, *J. Chem. Phys.* **97**, 2920 (1992).
- <sup>13</sup>X. Song, E. R. Davidson, S. R. Gwaltney, and J. P. Reilly, *J. Chem. Phys.* **100**, 5411 (1994).
- <sup>14</sup>J. M. Smith and J. L. Knee, *Laser Chem.* **14**, 131 (1994).
- <sup>15</sup>M. C. R. Cockett, K. Okuyama, and K. Kimura, *J. Chem. Phys.* **97**, 4679 (1992).
- <sup>16</sup>D. Bahatt, A. Heidenreich, N. Ben-Horin, U. Even, and J. Jortner, *J. Chem. Phys.* **100**, 6290 (1994).
- <sup>17</sup>M. Itoh and Y. Morita, *J. Phys. Chem.* **92**, 5693 (1988).
- <sup>18</sup>M. Itoh and A. Hayashi, *J. Phys. Chem.* **93**, 7789 (1989).
- <sup>19</sup>A. R. Auty, A. C. Jones, and D. Phillips, *Chem. Phys.* **103**, 163 (1986).
- <sup>20</sup>L. Zhu and P. M. Johnson, *J. Chem. Phys.* **94**, 5769 (1991).
- <sup>21</sup>Xu Zhang and J. L. Knee, *Faraday Discuss.* **97**, 299 (1994); *Femtosecond Chemistry*, edited by Jörn Manz and Ludger Wöste (VCH Verlagsgesellschaft mbH, Weinheim, 1995), Chap. 4.
- <sup>22</sup>W. C. Wiley and I. H. McLaren, *Rev. Sci. Instrum.* **26**, 1150 (1955).
- <sup>23</sup>Hypercube, Waterloo, Ontario, Canada.
- <sup>24</sup>GAUSSIAN 94, Revision D.4, M. J. Frisch, G. W. Trucks, H. B. Schlegel, P. M. W. Gill, B. G. Johnson, M. A. Robb, J. R. Cheeseman, T. Keith, G. A. Petersson, J. A. Montgomery, K. Raghavachari, M. A. Al-Laham, V. G. Zakrzewski, J. V. Ortiz, J. B. Foresman, J. Cioslowski, B. B. Stefanov, A. Nanayakkara, M. Challacombe, C. Y. Peng, P. Y. Ayala, W. Chen, M. W. Wong, J. L. Andres, E. S. Replogle, R. Gomperts, R. L. Martin, D. J. Fox, J. S. Binkley, D. J. Defrees, J. Baker, J. P. Stewart, M. Head-Gordon, C. Gonzalez, and J. A. Pople, Gaussian, Inc., Pittsburgh PA, 1995.

<sup>25</sup>H. J. Neusser and H. Krause, *Chem. Rev.* **94**, 1829 (1994).

<sup>26</sup>P. Hobza, H. L. Selzle, and E. W. Schlag, *J. Chem. Phys.* **95**, 391 (1991).

<sup>27</sup>H. Koch, B. Fernandez, and O. Christiansen, *J. Chem. Phys.* **108**, 2784 (1998).

<sup>28</sup>S. F. Boys and F. Bernardi, *Mol. Phys.* **19**, 553 (1970).

<sup>29</sup>T. G. Wright, *J. Chem. Phys.* **105**, 7579 (1996); S. A. C. McDowell, *Chem. Phys. Lett.* **266**, 38 (1997); V. Subramanian, K. Venkatesh, D. M. Prabha, and T. Ramasami, *Chem. Phys. Lett.* **267**, 9 (1997).